

# Controlled vortex core switching in a magnetic nanodisk by a rotating field

Volodymyr P. Kravchuk,<sup>1</sup> Denis D. Sheka,<sup>1,\*</sup> Yuri Gaididei,<sup>2</sup> and Franz G. Mertens<sup>3</sup>

<sup>1</sup>*National Taras Shevchenko University of Kiev, 03127 Kiev, Ukraine*

<sup>2</sup>*Institute for Theoretical Physics, 03143 Kiev, Ukraine*

<sup>3</sup>*Physics Institute, University of Bayreuth, 95440 Bayreuth, Germany*

(Dated: 21.05.07)

The switching process of the vortex core in a Permalloy nanodisk affected by a rotating magnetic field is studied theoretically. A detailed description of magnetization dynamics is obtained by micromagnetic simulations.

PACS numbers: 75.10.Hk, 75.70.Ak, 75.40.Mg, 05.45.-a

Artificial mesoscopic magnetic structures provide now a wide testing area for concepts of nanomagnetism and numerous prospective applications [1, 2]. A remarkable example is a vortex state nanodot. Having nontrivial topological structure on a scale of a nanomagnet, magnetic vortex is a promising candidate for a high density magnetic storage and high speed magnetic random access memory [3]. The basis of the vortex statics and dynamics in Heisenberg magnets was studied in 1980s, for a review see Ref. [4]. Typically, the vortex is considered as a rigid particle without internal degrees of freedom. Using such an approach a number of dynamical effects were studied in Heisenberg magnets [4] and also in nanomagnets [5]. However, the rigid approach fails when considering the vortex dynamics under the influence of a strong or fast external force. In particular, it is known that external pumping excites internal modes in vortex dynamics in Heisenberg magnets, whose role is important for understanding the switching phenomena [6, 7, 8, 9, 10, 11], and the limit cycles in the vortex dynamics [12, 13].

In the present work we study the effect of influence of the homogeneous rotating field  $\mathbf{B}(t) = (B \cos \omega t, B \sin \omega t, 0)$  on nonlinear internal dynamics of the vortex state magnetic nanodot in the framework of Landau-Lifshitz-Gilbert equations with account of the exchange and dipolar interaction. Using micromagnetic simulations for material parameters of Permalloy (Py), [34] we found that the irreversible flipping process of the vortex core polarity  $p$  is possible in a specific range of the field parameters  $(B, \omega)$ , when the direction of  $\omega$  is opposite to the vortex polarity, i.e. when  $\omega p < 0$ .

The simplest way to flip the vortex can be realized by applying a perpendicular DC field  $B_\perp$ . Due to this field the heavy vortex, which is polarized against the field, becomes unstable [14, 15] and at some critical value ( $B_s \sim 1.5\pi M_S$  [16],  $M_S$  is the saturation magnetization [34]) it flips to the light vortex state in which the core magnetization is parallel to the field. Note that this switching field should be strong enough,  $B_s \sim 2.5$  kOe [16, 17, 18, 19]. Another possibility to switch the vortex is to use a weak but fast rotating field  $\mathbf{B}(t)$  [7, 8, 9, 10]. The physical idea is very simple. Let us consider our

system a moving frame, which rotates with a frequency  $\omega$  together with the field. In this frame instead of the rotating field one has a static in-plane field  $B$ . According to the Larmor theorem there appears also an effective perpendicular field  $B_\perp = \hbar\omega/(g\mu_B)$ . Thus the switching problem under the action of the AC field reduces to the problem with two DC fields. This idea perfectly works for the Heisenberg magnets and the dynamical picture of the switching is almost the same for both DC and AC field [10]. However, as we show in this letter, this simple picture fails for magnetic nanodots, where the dipolar interaction is decisive for the vortex structure [1, 2].

Probably the simplest way which gives physical insight how the dipolar interaction secures the stability of curling ground state is to use a local approach [20]. In this approach the dipolar interaction can be reduced approximately to an on-site anisotropy energy which in the case of a cylindrical nanodot has the form

$$\frac{E_{\text{dipolar}}}{\pi R^2 h M_S^2} \approx \int d^2 x \left[ \mathcal{A}(r) + \mathcal{B}(r) \cos 2(\phi - \chi) \right] \sin^2 \theta. \quad (1)$$

Here  $(r, \chi)$  are the polar coordinates in the XY plane and we use the angular parametrization for the magnetization  $M_x + iM_y = M_S \sin \theta \exp(i\phi)$  and  $M_z = M_S \cos \theta$ . For thin nanodots the easy-plane anisotropy parameter  $\mathcal{A}(r)$  is negative being practically a constant. The in-plane anisotropy parameter  $\mathcal{B}(r)$  is coordinate-dependent: it vanishes in the disk center and it is sharply localized near the disk edge [20]. One can see that for the easy-plane uniform state nanodot with  $\phi = \text{const}$ ,  $\theta = \pi/2$ , the second (in-plane) energy term in (1) vanishes after integration and makes no important contribution. However, for the vortex state

$$\cos \theta = pf \left( \frac{r}{\ell} \right), \quad \phi = q\chi + \aleph \frac{\pi}{2} \quad (2)$$

with  $q = 1$  being the vorticity and  $\aleph = \pm 1$  being the chirality,  $\cos 2(\phi - \chi) = -1$  and the dipolar interaction (1) is of crucial importance. In (2) an exponentially localized function  $f(r/\ell)$  describes the vortex core structure. For thin disks one can neglect the z-dependence of the magnetization [16]. The topological properties of

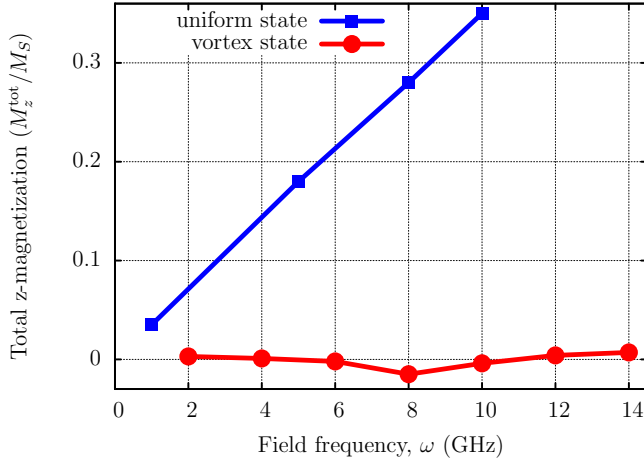


FIG. 1: (Color online) The ground state magnetization of the nanodot as a function of the AC field frequency: blue squares correspond to the uniform state nanodot (80 nm diameter, 2 nm thickness), red circles to the vortex state nanodot (132 nm diameter, 20 nm thickness). For both cases the field strength  $B = 0.05$  T.

the magnetization distribution are characterized by the Pontryagin index

$$Q = \frac{1}{4\pi} \int d^2x \mathcal{Q}, \quad \mathcal{Q} = \epsilon_{ij} \sin \theta \partial_i \theta \partial_j \phi. \quad (3)$$

For the vortex configuration (2) the Pontryagin index is  $Q = pq/2$ .

To study the vortex core dynamics in a nanoparticle we performed a detailed simulations, using the OOMMF micromagnetic simulator for Landau-Lifshitz-Gilbert equations [21]. We simulated the vortex state Py nanodisk [34] with the diameter  $2L = 132$  nm and the thickness  $h = 20$  nm.

First we decided to validate the analogy between the rotating AC field and effective DC field for the nanodot. Since the visual effect of the DC field is the change of the ground state magnetization, we calculated the dependence of  $M_z^{\text{tot}}$  on the frequency of the AC field  $\omega$ , see Fig. 1. For the uniform state nanodot, the dependence is linear,  $M_z^{\text{tot}} = \hbar\omega/(4\pi g\mu_B)$ , hence the analogy with the effective static field  $B_{\perp}$  works correctly for this case. However it fails for the vortex state nanodot, where  $M_z^{\text{tot}} \approx 0$ , see Fig. 1. The reason for this is the following. While in infinite systems the transformation to the rotating frame of reference in the space of spin variables ( $\phi \rightarrow \tilde{\phi} = \phi + \omega t$ ) makes the Hamiltonian of the system time independent, this is not the case in finite-size systems. As is seen from (1) (and takes place also for the total dipole-dipole interaction) to produce a time independent Hamiltonian in addition to the spin transformation one should transfer to the rotating frame of reference in real space:  $\chi \rightarrow \tilde{\chi} = \chi + \omega t$ . Thus in the rotating frame one has a static magnetic field  $\mathbf{B}$  along one axis in a disk plane. Besides that, taking into account that the

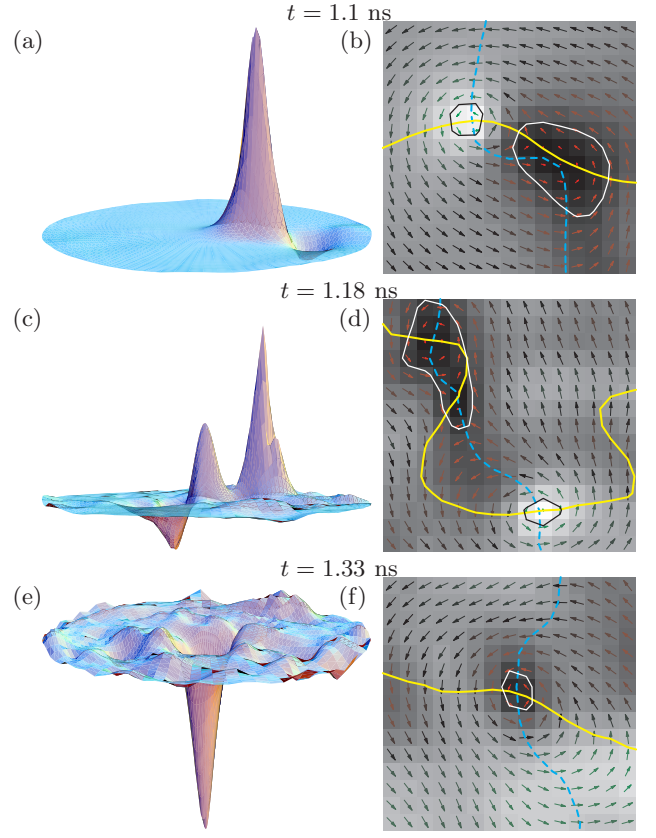


FIG. 2: (Color online) The temporal picture of the vortex switching process for the 132 nm diameter and 20 nm thickness Py disk: the left panel [Figs. (a), (c), (e)] corresponds to the 3D distribution of the topological density  $\mathcal{Q}$ , see Eq. (3), and the right panel [Figs. (b), (d), (f)] represents the in-plane magnetization distribution. The dashed blue and the solid yellow curves represent  $M_y = 0$  and  $M_x = 0$  isosurfaces, respectively; the black and the white curves correspond to  $M_z/M_S = 0.75$  and  $M_z/M_S = -0.75$  isosurfaces, respectively. The field parameters:  $\omega = 4$  GHz and  $B = 0.06$  T.

Lagrangian of the system contains a gyroscopical term of the form  $\int d^2x (p - \cos \theta) \partial_t \phi$ , [22] the Larmor and gyroscopical terms provide an additional energy contribution

$$\Delta E = \frac{M_S \hbar \omega}{\gamma} \int d^2\tilde{x} (p - \cos \theta) \left( 1 - \frac{\partial \tilde{\phi}}{\partial \tilde{\chi}} \right). \quad (4)$$

Without a vortex, the additional energy term (4) is equivalent to the action of an effective perpendicular magnetic field,  $\Delta E = -B_{\perp} M_z^{\text{tot}}$ , which results in a not vanishing  $M_z^{\text{tot}}$ , in accordance with above results, see Fig. 1. If the vortex is present, the situation drastically changes. In particular,  $\Delta E = 0$  for the vortex which is situated exactly in a disk center. This explains why we do not have an essential field influence on a centered vortex.

If we apply the field, which rotates clockwise ( $\omega < 0$ ), the vortex with  $p = +1$  starts to move counterclockwise. This vortex motion has a gyroscopical nature: the vortex trajectory  $\mathbf{R}(t)$  results mainly from the balance between

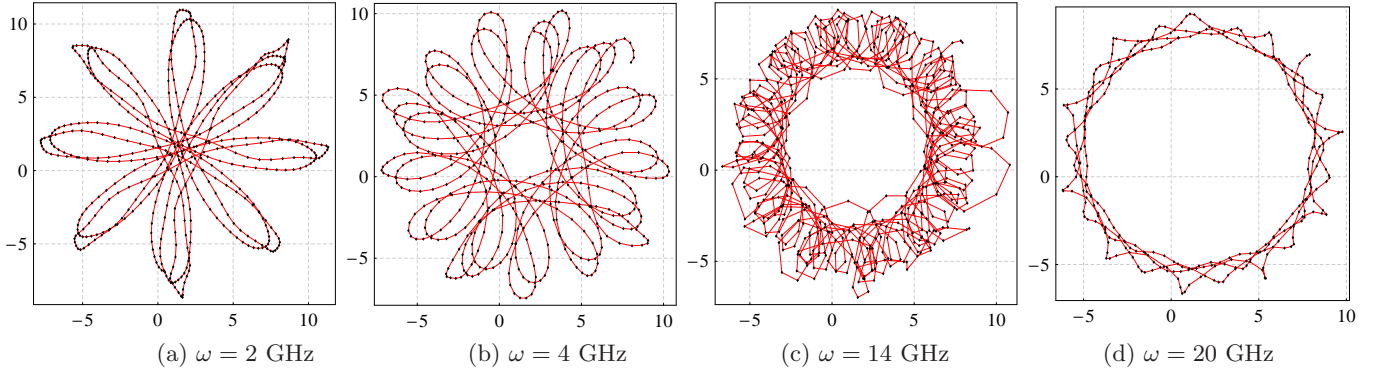


FIG. 3: (Color online) Vortex trajectories (measured in nanometers) for different frequencies. The field amplitude always is the same (0.02T).

the field interaction and the internal gyroscopic force  $\mathbf{G} \times d\mathbf{R}/dt$ , where  $\mathbf{G} = -4\pi M_S h \gamma^{-1} Q \mathbf{e}_z$  is the gyrovector.

During its motion, the vortex excites a number of spin waves [23], the vortex trajectory becomes complicated and sometimes it is tricky to identify the exact vortex position. We used the spatial distribution (3) of the topological density  $Q$ , to determine the vortex center position  $\mathbf{R}(t)$ . This distribution of  $Q$  is shown on the left panel of Fig. 2. Typical vortex trajectories are shown in Fig. 3. Mainly two magnon modes are excited in this system: symmetrical and azimuthal ones [7, 10]. The azimuthal mode is caused by the influence of the in-plane field and the symmetrical one by the effective out-of plane field  $B_\perp$ . Due to the continuous pumping the system goes to the nonlinear regime: the amplitude of the azimuthal mode increases and there appears an out-of-plane dip nearby the vortex, similar to the vortex structure distortion by the in-plane field pulse [24, 25, 26] or an AC oscillating field [27]; this dip is shown on the right panel of Fig. 2 by the dark gray color and it is surrounded by the white isosurface. To highlight the vortex core position on the XY plane (right panel of Fig. 2), we plot the isosurfaces  $M_x = 0$  and  $M_y = 0$ : each intersection of these isosurfaces determines the position of the vortex ( $q = +1$ ) or the antivortex ( $q = -1$ ) [24]. All isosurfaces are closed inside the disk, or go the disk edge, hence the number of crossing points can be changed during the system dynamics only by two, reflecting the processes of the vortex-antivortex pair creation and annihilation.

When the amplitude of the out-of-plane dip reaches the minimum ( $M_z = -M_S$ ) a pair of a *new* vortex ( $p = -1$ ,  $q = +1$ ) and antivortex ( $p = -1$ ,  $q = -1$ ) is created, see Figs. 2 (c) and (d). Since the total topological charge of the pair  $Q = 0$ , this process does not cost a lot of energy [28]. On Fig. 2(c) one can see three peaks in the  $Q$ -distribution. Two positive peaks correspond to the initial vortex and the new antivortex. The negative peak corresponds to the new vortex. After that the scenario of the vortex-vortex-antivortex dynamics is similar to the one discussed by Waeyenberge et al. [25]. The original vortex

and the new antivortex interact with each other. In the exchange limit (neglecting the dipolar interaction) the vortex-antivortex pair is topologically equivalent to the Belavin-Polyakov soliton [29] with the topological charge  $Q = 1$ . This soliton is scale invariant in the continuum system. However, in the discrete system the radius of this soliton, i.e. the distance between the vortex and antivortex, rapidly decreases almost without energy lost, since this soliton is not stable. When the soliton radius is about the lattice constant, it can vanishes; this vanishing is accompanied by strong spin-wave radiation, because the topological properties of the system change [28, 30]. After annihilation of the vortex-antivortex pair only the new vortex ( $p = -1$ ) survives, see Figs. 2 (e) and (f). After the flipping the vortex changes the direction of motion, because it has now the opposite polarity. The interaction with the rotating field is not so strong now, and the vortex rapidly goes to the disk center on a spiral trajectory. Thus, using the rotating field we obtain an *irreversible* switching of the vortex polarity. The Sup-

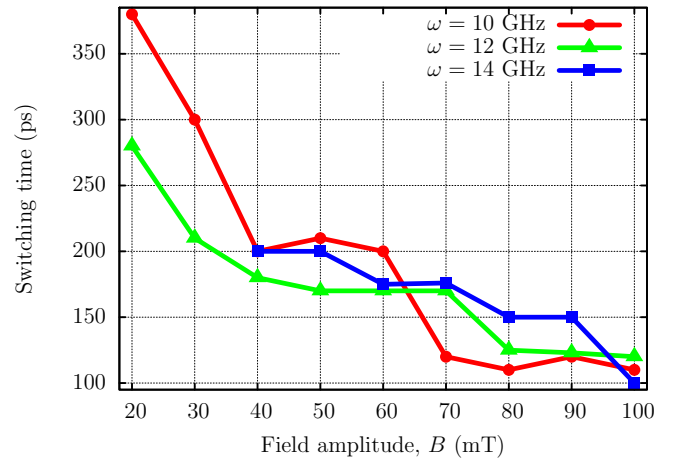


FIG. 4: (Color online) The switching time for different field parameters. The size parameters of the dots are the same as in Fig. 2

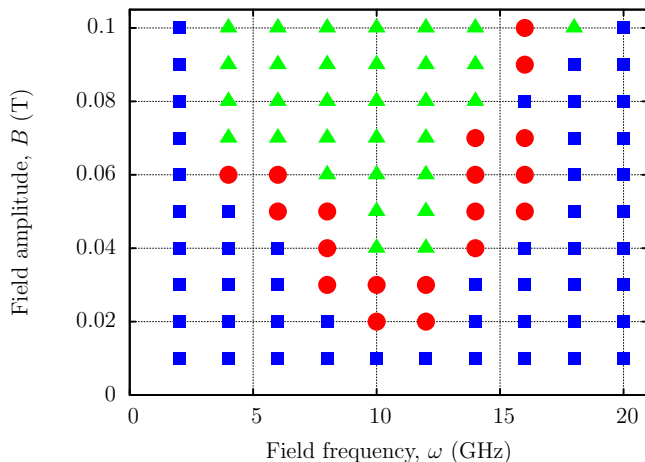


FIG. 5: (Color online) Switching diagram for the ac field parameters (amplitude and frequency): The symbols ● correspond to parameters, when the switching occurs, ■ describe the vortex dynamics without switching, and ▲ represent multiple switching processes.

plementary Video illustrates the whole evolution of the magnetization distribution during the switching process [35]. Typically the switching time is in the hundreds ps range; it can be decreased by more intensive fields, see Fig. 4 [36].

The switching occurs in a well defined range of the field parameters ( $\omega, B$ ) with the minimum frequency about 10 GHz and the field strength about 20 mT, see Fig. 5. When the field intensity is not strong enough, the vortex moves without switching. In the opposite case of strong fields, multiple switching occurs, similar to [24, 27]. When the frequency is too large or too small the switching also does not happen. Thus, the controlled switching process can be realized experimentally only for a relatively narrow range of parameters (red disks in the switching diagram, Fig. 5). The switching diagram differs from the one in Heisenberg magnets, where the vortex flipping is characterized mainly by a threshold curve  $B_{cr}(\omega)$  [7, 10].

Note that in the range of the high frequency pumping, when the switching does not occur (the right sight of the diagram 5), the vortex always reaches some limit cycle, which is almost a circular trajectory, see Fig. 3(d). An important feature of this limit cycle is that the frequency of the vortex orbital motion  $\Omega \sim 1$  GHz is much less than the pumping frequency  $\omega$  and almost does not depend on the field frequency and its amplitude. We expect that this low frequency response results from the coupling between the vortex motion and internal modes dynamics in analogue with the Heisenberg magnets [12, 13]. The detailed analysis of this vortex dynamics is under construction.

In conclusion, we have described the vortex core dynamics in the nanodisk under periodic driving. The ir-

reversible switching of the vortex polarity can be excited by a high-frequency (10 GHz) and intensity (20 mT) AC field. The mechanism of the switching involving the creation and annihilation of a vortex-antivortex pair is quite general. It appears for different kinds of vortex excitation and is induced in particular by a field pulse [25, 26, 31], by an AC oscillating field [27], and even by an electrical current [32, 33]. We also reported about the limit cycle in the vortex dynamics for the higher frequency pumping. Both effects are caused by the strong coupling with excited internal magnon modes.

The authors thank S. Komineas, H. Stoll and M. Fähnle for helpful discussions. V.K., D.S., Yu.G. thank the University of Bayreuth, where this work was performed, for kind hospitality and acknowledge the support from DLR grant No. UKR 05/055. V.K. acknowledges the support from the BAYHOST project. D.S. acknowledges the support from the Alexander von Humboldt-Foundation.

---

\* Corresponding author. Electronic address: denis\_sheka@univ.kiev.ua

- [1] A. Hubert and R. Schäfer, *Magnetic domains* (Springer-Verlag, Berlin, 1998).
- [2] R. Skomski, *J. Phys. C* **15**, R841 (2003), URL <http://www.iop.org/EJ/abstract/0953-8984/15/20/202/>.
- [3] R. P. Cowburn, *J. Magn. Magn. Mater.* **242-245**, 505 (2002), URL <http://www.sciencedirect.com/science/article/B6TJJ-44NM486-19/2/d76afadecc91907bb34369038cc8368e>.
- [4] F. G. Mertens and A. R. Bishop, in *Nonlinear Science at the Dawn of the 21th Century*, edited by P. L. Christiansen, M. P. Soerensen, and A. C. Scott (Springer-Verlag, Berlin, 2000).
- [5] K. Y. Guslienko, B. A. Ivanov, V. Novosad, Y. Otani, H. Shima, and K. Fukamichi, *J. Appl. Phys.* **91**, 8037 (2002), URL <http://link.aip.org/link/?JAP/91/8037/1>.
- [6] Y. Gaididei, T. Kampeter, F. G. Mertens, and A. Bishop, *Phys. Rev. B* **59**, 7010 (1999), URL <http://link.aps.org/abstract/PRB/v59/p7010>.
- [7] Y. Gaididei, T. Kampeter, F. G. Mertens, and A. R. Bishop, *Phys. Rev. B* **61**, 9449 (2000), URL <http://link.aps.org/abstract/PRB/v61/p9449>.
- [8] A. S. Kovalev and J. E. Prilepsky, *Low Temp. Phys.* **28**, 921 (2002).
- [9] A. S. Kovalev and J. E. Prilepsky, *Low Temp. Phys.* **29**, 55 (2003).
- [10] J. P. Zagorodny, Y. Gaididei, F. G. Mertens, and A. R. Bishop, *Eur. Phys. J. B* **31**, 471 (2003), URL <http://dx.doi.org/10.1140/epjb/e2003-00057-y>.
- [11] J.-G. Caputo, Y. Gaididei, F. G. Mertens, and D. D. Sheka, *Phys. Rev. Lett.* **98**, 056604 (pages 4) (2007), URL <http://link.aps.org/abstract/PRL/v98/e056604>.
- [12] J. P. Zagorodny, Y. Gaididei, D. D. Sheka, J.-G. Caputo, and F. G. Mertens, *Phys. Rev. Lett.* **93**, 167201 (pages 4) (2004), URL <http://link.aps.org/abstract/PRL/v93/>



- e167201.
- [13] D. D. Sheka, J. P. Zagorodny, J. G. Caputo, Y. Gaididei, and F. G. Mertens, Phys. Rev. B **71**, 134420 (pages 15) (2005), URL <http://link.aps.org/abstract/PRB/v71/e134420>.
  - [14] B. A. Ivanov and D. D. Sheka, Low Temp. Phys. **21**, 881 (1995), URL <http://link.aip.org/link/?LTP/21/881/1>.
  - [15] B. A. Ivanov and G. M. Wysin, Phys. Rev. B **65**, 134434 (pages 17) (2002), URL <http://link.aps.org/abstract/PRB/v65/e134434>.
  - [16] V. P. Kravchuk and D. D. Sheka, Physics of the Solid State **49**, (accepted) (2007).
  - [17] N. Kikuchi, S. Okamoto, O. Kitakami, Y. Shimada, S. G. Kim, Y. Otani, and K. Fukamichi, J. Appl. Phys. **90**, 6548 (2001), URL <http://link.aip.org/link/?JAP/90/6548/1>.
  - [18] T. Okuno, K. Shigeto, T. Ono, K. Mibu, and T. Shinjo, J. Magn. Magn. Mater. **240**, 1 (2002), URL <http://www.sciencedirect.com/science/article/B6TJJ-447DCMV-3/2/84e9fdfbf9e0cab3d3182fc4db4b4032>.
  - [19] A. Thiaville, J. M. Garcia, R. Dittrich, J. Miltat, and T. Schrefl, Phys. Rev. B **67**, 094410 (pages 12) (2003), URL <http://link.aps.org/abstract/PRB/v67/e094410>.
  - [20] J.-G. Caputo, Y. Gaididei, V. P. Kravchuk, F. G. Mertens, and D. D. Sheka, *Effective anisotropy of thin nanomagnets: beyond the surface anisotropy approach* (2007), arXiv:0705.1555, URL <http://arxiv.org/abs/0705.1555>.
  - [21] *The Object Oriented MicroMagnetic Framework*, developed by M. J. Donahue and D. Porter mainly, from NIST. We used the 3D version of the 1.2 $\alpha$ 2 release, URL <http://math.nist.gov/oommf/>.
  - [22] D. D. Sheka, Journal of Physics A: Mathematical and General **39**, 15477 (2006), URL <http://stacks.iop.org/0305-4470/39/15477>.
  - [23] S. Choi, K.-S. Lee, K. Y. Guslienko, and S.-K. Kim, Physical Review Letters **98**, 087205 (pages 4) (2007), URL <http://link.aps.org/abstract/PRL/v98/e087205>.
  - [24] R. Hertel, S. Gliga, M. Fahnle, and C. M. Schneider, Physical Review Letters **98**, 117201 (pages 4) (2007), URL <http://link.aps.org/abstract/PRL/v98/e117201>.
  - [25] V. B. Waeyenberge, A. Puzic, H. Stoll, K. W. Chou, T. Tylliszczak, R. Hertel, M. Fahnle, H. Bruckl, K. Rott, G. Reiss, et al., Nature **444**, 461 (2006), ISSN 0028-0836, URL <http://dx.doi.org/10.1038/nature05240>.
  - [26] Q. F. Xiao, J. Rudge, B. C. Choi, Y. K. Hong, and G. Donohoe, Applied Physics Letters **89**, 262507 (pages 3) (2006), URL <http://link.aip.org/link/?APL/89/262507/1>.
  - [27] K.-S. Lee, K. Y. Guslienko, J.-Y. Lee, and S.-K. Kim, *Ultrafast vortex-core reversal dynamics in ferromagnetic nanodots* (2007), cond-mat/0703538, URL <http://www.arxiv.org/abs/cond-mat/0703538>.
  - [28] O. A. Tretiakov and O. Tchernyshyov, Physical Review B (Condensed Matter and Materials Physics) **75**, 012408 (pages 2) (2007), URL <http://link.aps.org/abstract/PRB/v75/e012408>.
  - [29] A. A. Belavin and A. M. Polyakov, JETP Lett. **22**, 245 (1975).
  - [30] R. Hertel and C. M. Schneider, Phys. Rev. Lett. **97**, 177202 (pages 4) (2006), URL <http://link.aps.org/abstract/PRL/v97/e177202>.
  - [31] R. Hertel, S. Gliga, M. Fahnle, and C. M. Schneider, *Turning magnetic vortex cores upside down: Nanomagnetic toggle switching of vortex cores on the picosecond time scale* (2006), URL <http://arxiv.org/abs/cond-mat/0611668>.
  - [32] K. Yamada, S. Kasai, Y. Nakatani, K. Kobayashi, H. Kohn, A. Thiaville, and T. Ono, Nat Mater **6**, 270 (2007), ISSN 1476-1122, URL <http://dx.doi.org/10.1038/nmat1867>.
  - [33] Y. Liu, S. Gliga, R. Hertel, and C. M. Schneider, *Current-induced magnetic vortex core switching in a permalloy nanodisk* (2007), URL <http://www.arXiv.org/cond-mat/0702048>.
  - [34] In all simulations we used material parameters adopted for the Py particle: the exchange constant  $A = 1.3 \times 10^{-6}$  erg/cm, the saturation magnetization  $M_S = 8.6 \times 10^2$  G, the damping coefficient  $\alpha = 0.006$  and the anisotropy was neglected. This corresponds to the exchange length  $\ell = \sqrt{A/4\pi M_S^2} \approx 5.3$  nm, which determines the typical radius of the vortex core. The mesh cells have sizes  $3 \times 3 \times 20$  nm.
  - [35] Supplemental video, <http://www.phy.uni-bayreuth.de/~btp315/publ/Kravchuk.arXiv.0705.2046.html>
  - [36] In our simulations the vortex was initially shifted from the disk center on a distance about its core radius. The switching time slightly increases when we place the vortex exactly into the disk center.